

# 50 Joint Explorations, 1985-2007

Wm. G. Hoover and Carol G. Hoover

Highway Contract 60, Box 565

Ruby Valley, Nevada 89833

and Harald A. Posch

Institute for Experimental Physics

Universität Wien

Boltzmanngasse 5

Wien A-1090 Austria

(Dated: March 7, 2007)

## Abstract

Our joint explorations of microscopic and macroscopic physics are reviewed, on the occasion of a special meeting of the Schrödinger Institute honoring the 65th Birthday of Harald Posch.

PACS numbers: 05.20.-y, 05.45.-a, 07.05.Tp, 46, 05.70.Ln

Keywords: Thermostats, Fractals, Irreversibility, Lyapunov Instability, Smooth Particles

## I. INTRODUCTION

A quick count reveals that our 50 joint papers exceeds substantially (in both senses) the extent of our work with other authors. On this anniversary occasion a brief review is very much in order. We summarize our work in three main areas. We begin with applications and extensions of Shuichi Nosé’s pioneering approach, which included temperature and thermostats in mechanics. Next, comes our work on characterizing Lyapunov instability, and its applications to fractal geometry and the macroscopic irreversibility described by the Second Law. Last, comes our joint efforts in macroscopic simulation, to a large extent using particle-based smooth-particle methods influenced by our microscopic studies. The overall theme of this work is the linking together of microscopic mechanical concepts with macroscopic thermodynamics and hydrodynamics. This linkage is based on applying and extending Gibbs’ and Boltzmann’s ideas, which originated in the United States and here in Austria more than 100 years ago.

## II. MECHANICS WITH TEMPERATURE AND THERMOSTATS, 1985-2007

The late Shuichi Nosé’s 1984 discovery of thermostated mechanics opened up a wide area for exploration. We assimilated and extended his work by applying it to a host of equilibrium and nonequilibrium systems. The simplest of them, a canonical-ensemble harmonic oscillator at equilibrium<sup>1</sup>, provided not only a variety of regular periodic solutions, but also Lyapunov-unstable chaotic solutions of the three simple motion equations:

$$\dot{q} = p ; \dot{p} = -q - \zeta p ; \dot{\zeta} = (p^2 - 1)/\tau^2 .$$

The friction coefficient  $\zeta$  and the thermal relaxation time  $\tau$  are the two new features introduced by Nosé. We generated projections and sections of the intricate phase-space structures ( in three dimensions,  $\{ q, p, \zeta \}$ , not just two ). These developed overnight on a computer screen in Harald’s Boltzmannngasse office. The next morning, a dignified gentlemen in a white coat, bearing a large camera, was summoned. He photographed the computer screen for us. See Figure 1, for a sample  $( p, \zeta )$ -plane “Poincaré section” cut at  $q = 0$ .

The prominent “holes” in the cross section of Figure 1 are occupied by regular nonchaotic regions surrounding periodic orbits. One such periodic orbit is shown in Figure 2. For a

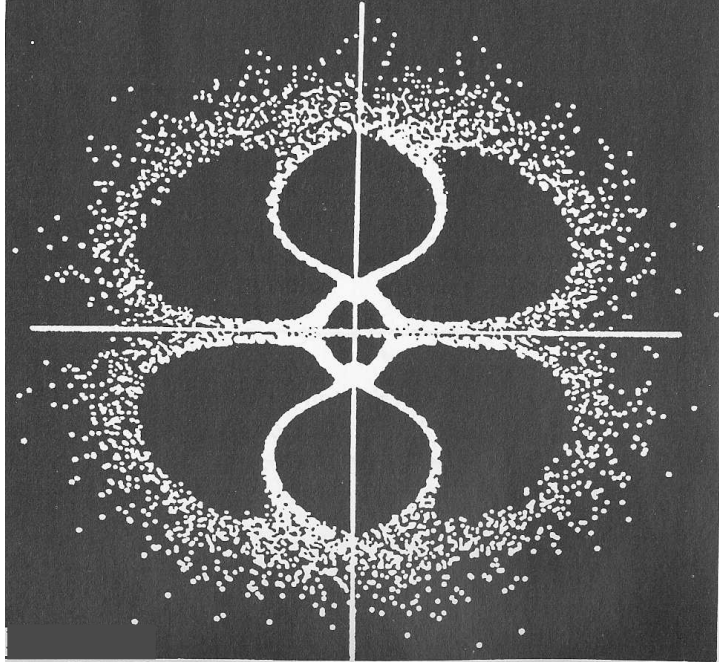


FIG. 1: Chaotic Poincaré section ( $q = 0$ ) for the Nosé-Hoover oscillator, from Reference 1.

fixed value of the thermostat timescale relaxation time  $\tau$  the sum total of all the regular orbits plus the chaotic one is the simple equilibrium Gaussian distribution,

$$f(q, p, \zeta) \propto e^{-[q^2+p^2+(\tau\zeta)^2]/2} .$$

Over 50 computer-generated pictures illustrating such models appear in our 1985 manuscript on the canonical dynamics of the Nosé oscillator<sup>1</sup>. WGH was then in Wien to work with Karl Kratky on hard-disk and hard-sphere transport problems, but ended up doing even more work with HAP, along with writing a book, “Molecular Dynamics”, describing a series of lectures presented during that visit<sup>2</sup>. A mature extended version of the subject matter, “Computational Statistical Mechanics”, appeared six years later<sup>3</sup>.

In the two decades since this pioneering work, applications of Nosé’s thermostat idea have been extended to [1] control of *stress*, as well as temperature; [2] control of *configurational* temperature, as well as kinetic temperature; [3] simultaneous control of higher moments than  $\langle p^2 \rangle$  or  $\langle F^2 \rangle$ , such as  $\langle p^4 \rangle$  by using *multiple controls*, which promote ergodicity; [4] temperature control for a wide variety of diffusive, shear, and heat flows in one, two, and three dimensions; [5] a geometric understanding of phase-space irreversibility; and [6] a solid theoretical embedding of the macroscopic notions of temperature and stress into traditional time-reversible Lagrangian and Hamiltonian microscopic mechanics.

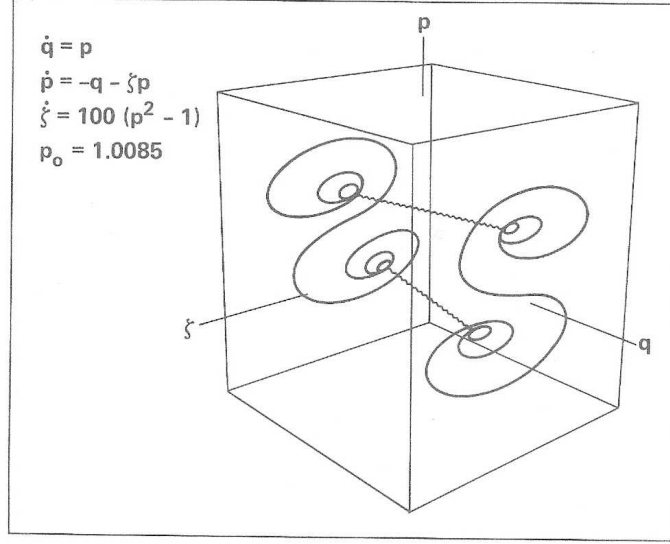


FIG. 2: A regular periodic orbit in  $(q, p, \zeta)$  space, for the Nosé-Hoover oscillator, with  $\tau = 0.1$ , taken from Reference 1.

This last application, the explicit introduction of temperature into microscopic mechanics provided a link, unknown to Boltzmann and Gibbs, which was instrumental in connecting the microscopic and macroscopic points of view. Very recently Dettmann and Morriss<sup>4</sup> discovered a direct link between Nosé's mechanics and Hamiltonian mechanics:

$$\mathcal{H} = \frac{K(p)}{s} + s \left[ \Phi(q) + \frac{1}{2}(\zeta\tau)^2 + \#kT \ln s \right] \equiv 0 .$$

Note the unusual, but crucial, trick of choosing a fixed value for the Hamiltonian. Without this choice, this approach would fail.

Even more recently Travis and Braga<sup>5-7</sup> used Liouville's Theorem for the flow of phase-space probability density  $f(q, p, \zeta, t)$ ,

$$\frac{\dot{f}}{f} \equiv - \left( \frac{\partial \dot{\zeta}}{\partial \zeta} \right) - \sum \left[ \left( \frac{\partial \dot{q}}{\partial q} \right) + \left( \frac{\partial \dot{p}}{\partial p} \right) \right] ;$$

$$\left[ \left( \frac{\partial f}{\partial t} \right) = 0 \right] \longrightarrow f(\{q, p\}, \zeta) \propto e^{-(\mathcal{H}/kT) - (\#\zeta^2\tau^2/2)} ,$$

to develop a *configurational* analog of the kinetic Nosé-Hoover thermostat. Here  $\#$  is the number of  $(q, p)$  degrees of freedom describing the system. This approach makes use of Landau and Lifshitz' classic identity<sup>8,9</sup> (from the canonical ensemble):

$$kT \equiv \frac{\langle F^2 \rangle}{\langle \nabla^2 \mathcal{H} \rangle} .$$

Applied to a simple harmonic oscillator (with force constant, mass, and temperature all equal to unity) the Travis-Braga configurational equations of motion (with the Landau-Lifshitz definition of temperature) are:

$$\dot{p} = -q ; \dot{q} = +p - \zeta q ; \dot{\zeta} = (q^2 - 1)/\tau^2 ; kT = 1 = \langle q^2 \rangle .$$

Recall now that the usual Nosé-Hoover equations of motion (with the kinetic definition of temperature) are:

$$\dot{q} = +p ; \dot{p} = -q - \zeta p ; \dot{\zeta} = (p^2 - 1)/\tau^2 ; kT = 1 = \langle p^2 \rangle .$$

Evidently the solutions of these two sets of equations, Travis-Braga and Nosé-Hoover, are *identical* once the substitutions  $+q \leftrightarrow -p$  are made.

### III. MECHANICAL INSTABILITY, FRACTALS, AND THE SECOND LAW, 1987-2002

Characterizing the chaotic solutions for the Nosé oscillator and its generalizations led us to seek, and find, an analytic representation for an algorithm generating the “Lyapunov spectrum”<sup>10</sup>. This spectrum of exponents, one for each phase-space dimension, gives the set of growth and decay rates,  $\propto e^{\lambda t}$ , of an infinitesimal comoving, corotating phase-space hypersphere centered on a trajectory satisfying the motion equations. Figure 3 shows the growth in the squared separation of two nearby phase-space trajectories over 3500 computational timesteps, starting at about  $(e^{-11})^2$  and reaching  $(e^{-3})^2$ . The underlying cell-model system is a single particle, moving in two-dimensional space and confined by four fixed neighboring particles. The slope of this semilogarithmic plot, when time-averaged and divided by  $2dt$ , is the largest Lyapunov exponent  $\lambda_1$ .

The idea underlying our work on the Lyapunov analysis was to use an array of Lagrange multipliers  $\{\lambda_{ij}\}$ , to stabilize the orthonormal arrangement of a comoving corotating set of basis vectors  $\{\delta_i\}$  in the phase space:

$$\{ \dot{\delta}_j(\mathcal{H}_0, \{\lambda\}) = \dot{\delta}_j(\mathcal{H}_0) - \sum_{i \leq j} \lambda_{ij}(t) \delta_i \} .$$

The time-averaged diagonal elements of the Lagrange-multiplier array turn out to correspond to the conventional Lyapunov spectrum:

$$\{ \langle \lambda_{ii}(t) \rangle \} \equiv \{ \lambda_i \} .$$

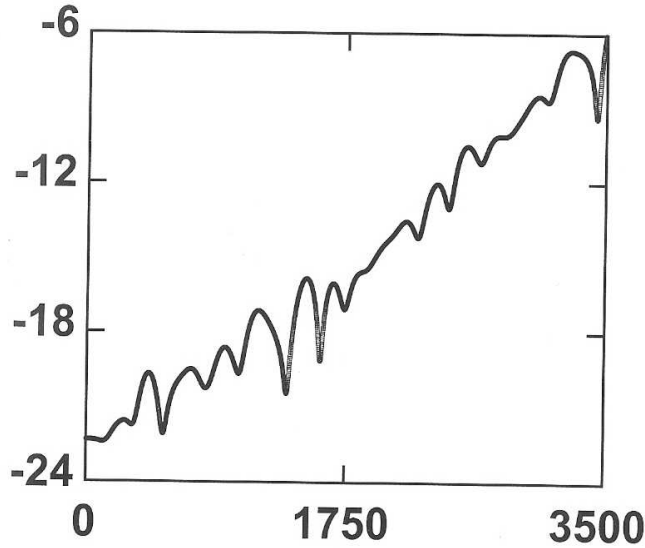


FIG. 3: Time dependence, for 3500 timesteps, of  $\ln(\delta_x^2 + \delta_y^2 + \delta p_x^2 + \delta p_y^2)$  for a two-dimensional nonlinear oscillator problem. The growth of the offset between two nearby phase-space trajectories gives the largest Lyapunov exponent for the problem.

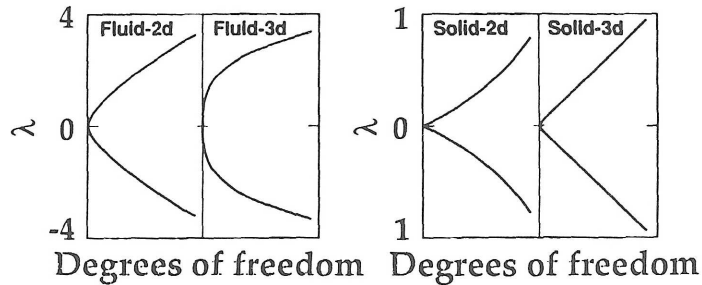


FIG. 4: Typical manybody Lyapunov spectra for two- and three-dimensional fluids and solids at equilibrium. There are two exponents, one positive and one negative, for each degree of freedom.

The Lagrange Multiplier approach makes it unnecessary to rescale the lengths of the  $\{\delta\}$ :

$$\{ \lambda_{ij}(t) \} \longrightarrow \{ \dot{\delta} \cdot \delta \equiv 0 \} .$$

Otherwise, the main advantage of this point of view is pedagogical, as Benettin's original method<sup>11</sup>, using rescaling of the comoving and corotating  $\{ \delta_j \}$ , is actually *more* efficient than using Lagrange multipliers for systems with more than a few phase-space dimensions.

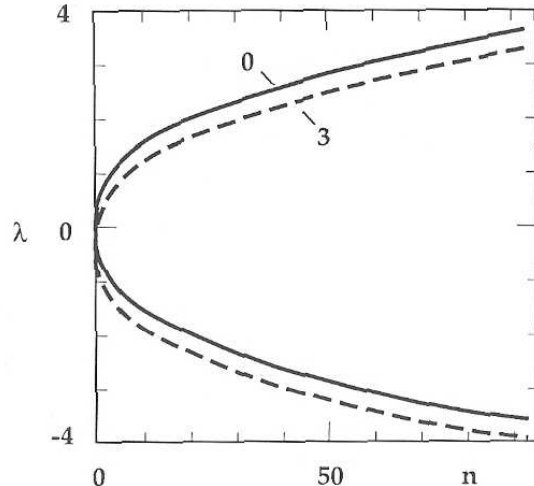


FIG. 5: Symmetry breaking for a stationary nonequilibrium state, thermostated and driven by an external field of strength 3. There are 32 three-dimensional particles (96 pairs of exponents). The corresponding exponent shift (from the solid line to the broken line) is roughly  $-0.8$  for each pair of exponents, and corresponds to a total dimensionality loss of  $-32$ , so that the dimensionality of the nonequilibrium strange attractor is about 164.

Computational advances did make it possible to characterize complete manybody spectra for both equilibrium and nonequilibrium systems. Figure 4 shows four such typical equilibrium Lyapunov spectra. These early equilibrium manybody spectra resemble simple power laws. A significant result, which took years to understand, was the *nonequilibrium* symmetry-breaking, corresponding to a negative shift of the spectrum. See Figure 5. This nonequilibrium work was presented in 1987 at a very pleasant meeting in southern Italy<sup>12</sup>, where the water, wine, and electricity flowed only intermittently, despite the high cost of the rooms.

Nosé's mechanics made it possible to show, analytically, that the exponents' shift was directly related to the entropy production of the external reservoirs represented by the thermostating forces:

$$\sum \lambda = -\frac{\dot{f}}{f} = \frac{\dot{\otimes}}{\otimes} = -\frac{\dot{S}_{\text{res}}}{k} < 0 .$$

The Second Law of Thermodynamics,  $\langle \dot{S}_{\text{res}} \rangle > 0$ , gave the paradoxical result that the phase volume  $\otimes$  representing a nonequilibrium steady state vanished! This shrinking<sup>13</sup>, to zero phase volume, was initially quite surprising given the time-reversible nature of the motion

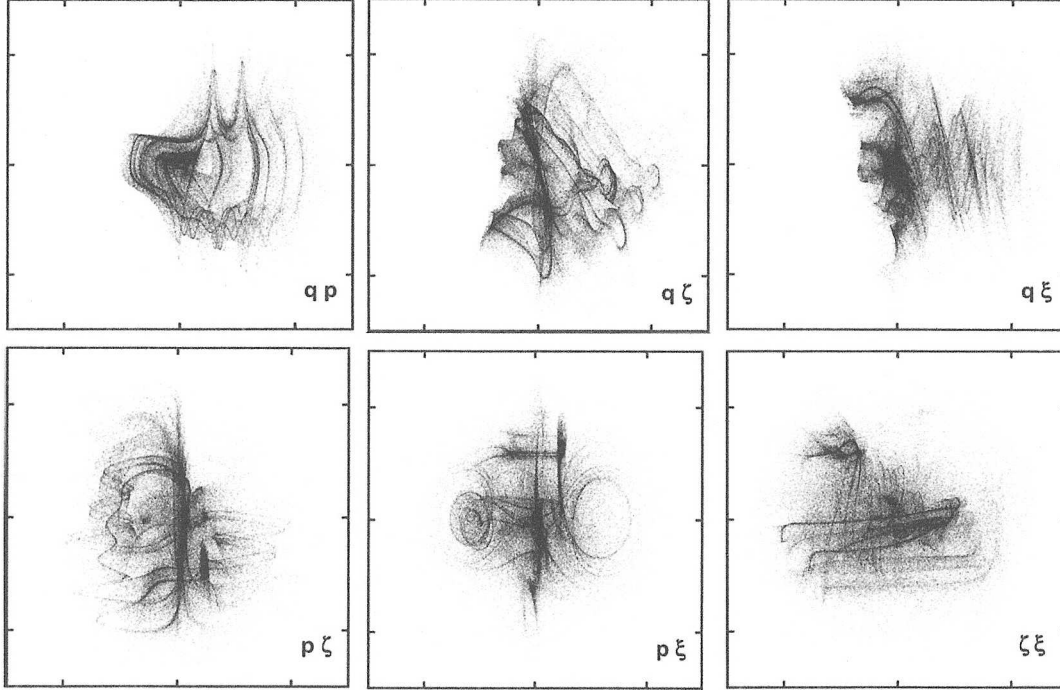


FIG. 6: Six projections of the 2.56-dimensional strange attractor for a nonequilibrium oscillator. The nonequilibrium temperature,  $T = 1 + \tanh(q)$ , leads to an overall transfer of heat from positive to negative values of the coordinate  $q$ . Analysis of this model provided definite evidence for the failure of the Kaplan-Yorke conjecture. See Reference 15.

equations, even away from equilibrium. The amazing coexistence of time-reversible equations with irreversible macroscopic behavior led to the book “Time Reversibility, Computer Simulation, and Chaos”<sup>14</sup>.

The analysis of Lyapunov spectra helps to explain the extreme rarity of nonequilibrium steady states in terms of phase-space dimensionality loss. In understanding this connection simple models have proved useful. The *doubly*-thermostated oscillator,

$$\dot{q} = p ; \dot{p} = -q - \zeta p - \xi p^3 ; \dot{\zeta} = p^2 - T ; \dot{\xi} = p^4 - 3p^2 T ; T = 1 + \epsilon \tanh(q) ,$$

where  $\zeta$  regulates  $p^2$  while  $\xi$  regulates  $p^4$ , is a specially instructive model. For  $\epsilon = 0$  this oscillator generates the four-dimensional Gaussian distribution,

$$f(q, p, \zeta, \xi) \propto e^{-[q^2 + p^2 + \zeta^2 + \xi^2]/2} .$$

For  $\epsilon = 1$  this oscillator generates a 2.56-dimensional nonequilibrium phase-space attractor. This directly-measured dimensionality, based on averaging  $f \ln f$  over up to  $128^4 = 2^{28}$

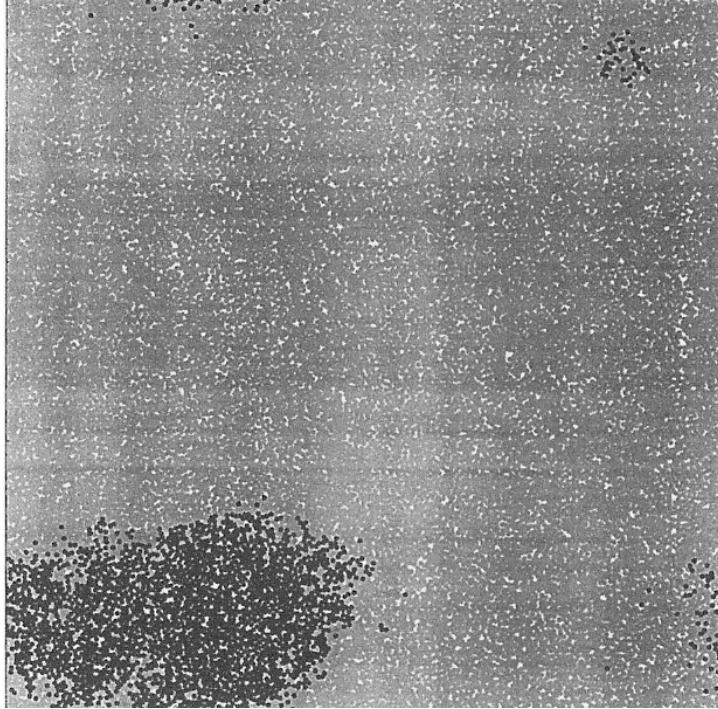


FIG. 7: Particle contributions to the largest Lyapunov exponent are indicated by shades of grey. Most of the contribution to the exponent is provided by only a few of the 25,600 particles in the lower left corner of the Figure. This mode is *localized* in physical  $(x, y)$  space. See Reference 16.

phase space bins, is in marked disagreement with the *estimated* information dimension of 2.80 based on Kaplan and Yorke's conjectured [and incorrect] relationship between the Lyapunov exponents and attractor dimensionality<sup>15</sup>. Two-dimensional projections of the attractor appear in Figure 6.

In considering the details of Lyapunov instability for manybody systems we noticed the very localized nature of the eigenvectors associated with the first few Lyapunov modes<sup>16</sup>. In some of his most important and seminal work Harald and his many coworkers found that modes near the middle of the Lyapunov spectrum, with small exponents, correspond to sinusoidal collective eigenvectors reminiscent of the sound and heat modes of ordinary hydrodynamics<sup>17</sup>. Figure 7 shows the localized nature of the first few (and last few) Lyapunov modes. This localized structure is qualitatively different to that of the modes corresponding to exponents near zero.

#### IV. CONTINUUM MECHANICS, 1995-2007

In 1977 two separate groups at Cambridge used *particle* methods to solve problems in *continuum* mechanics<sup>18</sup>. These “smooth particle” methods proved too intriguing for us to resist. They are a bridge between microscopic mechanics, governed by atomistic forces, and macroscopic mechanics, governed by thermodynamic and hydrodynamic constitutive relations. Because the approach is particularly simple and transparent, these methods are also ideal for students interested in solving continuum problems.

The smooth-particle equations of motion,

$$\{ \dot{v}_i = -m \sum_j \left[ \left( \frac{P}{\rho^2} \right)_i + \left( \frac{P}{\rho^2} \right)_j \right] \cdot \nabla_i w_{ij}(|r_{ij}|) \} ,$$

include a “weight” or “influence” function  $w_{ij}(|r_{ij}|)$ , a positive function with two continuous derivatives and a range of two or three particle spacings. The mass density  $\rho(r)$  at any point in space is computed by adding the contributions of all particles within the range of the weight function  $w(|r_{rj}|)$ :

$$\rho(r) \equiv \sum_j m_j w(|r_{rj}|) .$$

Spatial derivatives,

$$\{ \nabla \rho, \nabla v, \nabla T, \nabla \cdot P, \nabla \cdot Q \} ,$$

of the continuum variables needed for the righthandsides of the  $\{ \dot{\rho}, \dot{v}, \dot{e} \}$  equations,

$$\dot{\rho} = -\rho \nabla \cdot v ; \quad \rho \dot{v} = -\nabla \cdot P ; \quad \rho \dot{e} = -\nabla v : P - \nabla \cdot Q ,$$

all become simple sums over pairs of particles with the gradient operations replaced by differentiations of  $w$ . Because the components of  $\nabla w$  and  $\nabla \nabla w$  are simple (continuous) polynomials, this straightforward differentiation/interpolation procedure is simpler and faster than traditional finite-element approaches.

The smooth-particle approach can be applied to gases, liquids, or solids. The constitutive relations, which give the pressure tensor  $P$  and the heat flux vector  $Q$  in terms of the values, gradients, and time histories of  $\{ \rho, v, e \}$  distinguish one material from another. Notice that the special case of a two-dimensional ideal-gas constitutive relation,  $P \propto \rho^2$ , gives a continuum dynamics which corresponds to ordinary molecular dynamics with a pair potential  $w(r)$ . This similarity (isomorphic particle trajectories) made it possible<sup>19</sup> to shed light on the

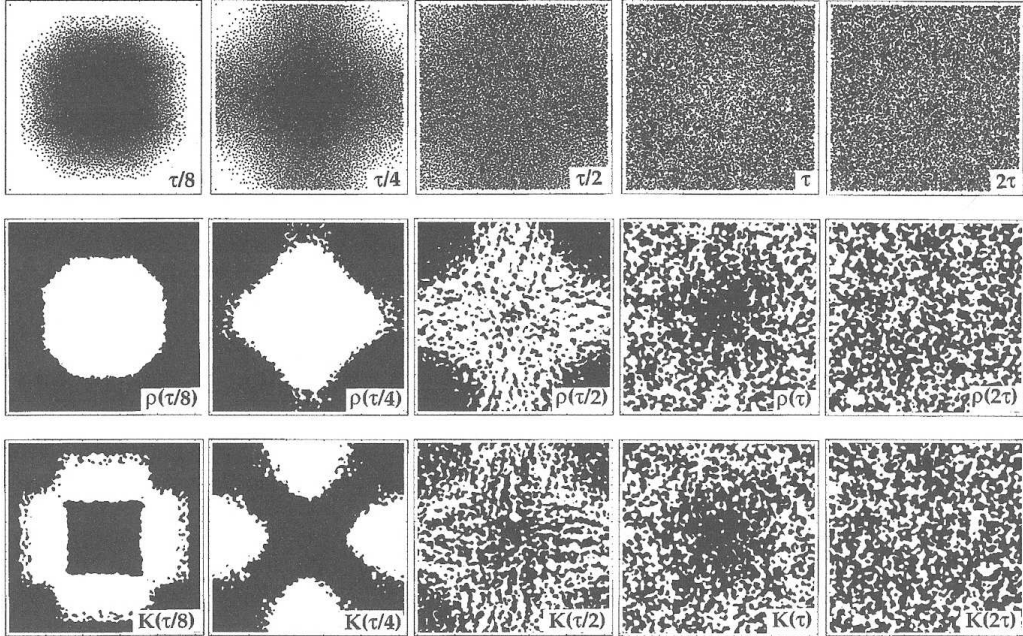


FIG. 8: The Figure shows (top) actual particle positions during five stages of a free expansion [  $\{\frac{\tau}{8}, \frac{\tau}{4}, \frac{\tau}{2}, \tau, 2\tau\}$ , where  $\tau$  is the sound traversal time ] together with the contour of mean density (middle) and mean kinetic energy (bottom). The fluctuations in these latter quantities “explain” the irreversibly-generated entropy increase associated with “Gibbs’ Paradox”. See Reference 19.

entropy increase associated with free expansions, tracing the entropy increase to fluctuations in the local velocity and density,

$$\langle v^2 \rangle \neq \langle v \rangle^2 ; \langle \rho^2 \rangle \neq \langle \rho \rangle^2 .$$

The smooth-particle version of the free expansion problem corresponds to the solution of the Euler equations, augmented by an artificial viscosity and artificial heat conductivity. Steady uniform Newtonian shear flows, and Fourier heat flows, can be used to study the convergence of the smooth-particle solutions to the analytic solutions which apply in the many-particle continuum limit<sup>20,21</sup>.

The Rayleigh-Bénard problem combines shear flow and heat flow. In this problem a fluid is heated from below. Solutions can provide a variety of flows depending upon the relative strength of the temperature gradient driving the motion (through the mechanism of thermal expansion). Although this problem involves both conductive and convective heat flows, numerical solutions are relatively easy to obtain because the boundaries and the boundary temperatures are fixed.

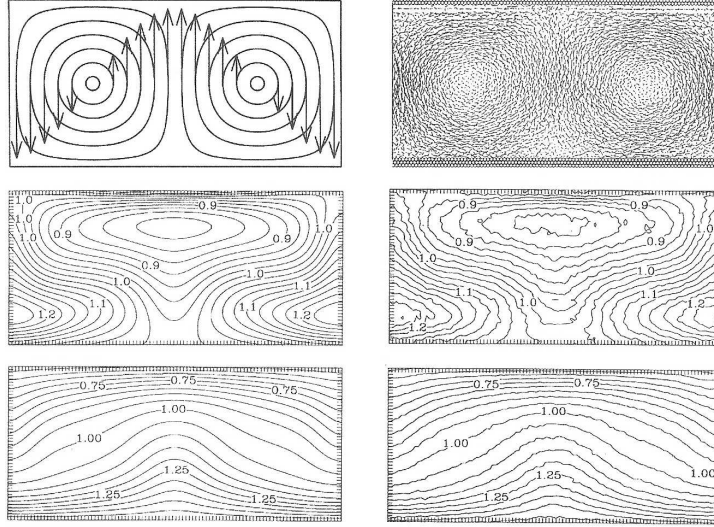


FIG. 9: A 5000-particle Rayleigh-Bénard simulation. The initial velocities and a typical particle snapshot appear at the top. The density and temperature contours calculated as instantaneous smooth-particle averages (right, center and bottom) are compared to accurate finite difference contours (left, center and bottom).

Figure 9 shows a relatively small-scale solution, using 5000 particles. Contours of density and temperature can be computed from a regular grid of points upon which the grid values are calculated as particle sums:

$$\rho(r) \equiv \sum_j m_j w(|r_{rj}|) ; T(r) \equiv \frac{\sum_j T_j w(|r_{rj}|)}{\sum_j w(|r_{rj}|)} .$$

Evidently the errors in the smooth-particle solution are on the order of one percent.

Similar grid-based sums can be used to compute Fourier transforms of all the hydrodynamic variables. This computational technique has tremendous advantages, both pedagogical and practical, when it comes to solving problems in continuum mechanics. Applications to flows and to fracture are many. Our work in this area led to a recently published book<sup>22</sup>.

We studied more complex two-dimensional “Kolmogorov flows” using smooth particles. These flows are driven by the usual smooth-particle version of the equations of motion,

$$\{ \dot{v}_i = -m \sum_j \left[ \left( \frac{P}{\rho^2} \right)_i + \left( \frac{P}{\rho^2} \right)_j \right] \cdot \nabla_i w_{ij}(|r_{ij}|) \} ,$$

with an additional sinusoidal acceleration added on,  $g(0, \sin(kx))$  or  $g(\sin(ky), 0)$ . Here  $g$  is the amplitude of the sinusoidal acceleration. Simulations with various aspect ratios, periodic

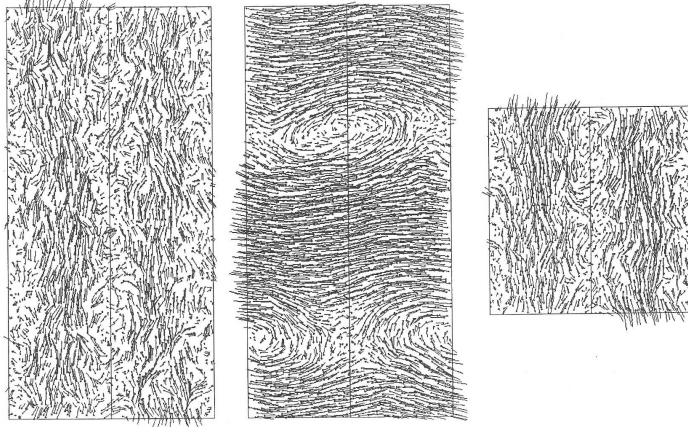


FIG. 10: Three views of “Kolmogorov flows”, field-driven periodic flows, which can be either regular or turbulent depending upon the strength of the driving force. The sinusoidal driving force is either vertical or horizontal in the views shown here. See Reference 23 for details.

in both the  $x$  and  $y$  directions, show clearly the transition from laminar to turbulent flow that occurs for sufficiently large  $g$ . Figure 10 illustrates three such flows.

Although by now *many* hydrodynamic simulations have been carried out using smooth-particle methods, there remains much to be done, particularly in developing constitutive relations for the application of these models to solid-phase flow and failure problems.

## V. CONCLUSIONS

Harald’s work with us has not only been enjoyable and intellectually valuable in itself. It has also been particularly seminal in advancing the interconnections linking statistical mechanics, nonlinear dynamics, and macroscopic hydrodynamics. As a result of his work we can implement control variables in microscopic simulations and can understand the connection of the microscopic control variables with macroscopic irreversible thermodynamics, We can also use particle methods to solve and understand relatively complex continuum problems in a simple way.

### Acknowledgments

These highspots of our joint work were presented in Vienna at the 18-20 April 2007 meeting, “Nonlinear Dynamics Meets Stochastic Dynamics”, which celebrated Harald Posch’s

65th Birthday. WGH and CGH very much appreciate the organizers' invitation to participate in that meeting.

---

- <sup>1</sup> H. A. Posch, W. G. Hoover, and F. J. Vesely, "Canonical Dynamics of the Nosé Oscillator: Stability, Order, and Chaos", *Physical Review A* **33**, 4253-4265 (1986)
- <sup>2</sup> Wm. G. Hoover, *Molecular Dynamics*, Lecture Notes in Physics **258** (Springer-Verlag, Berlin, 1986).
- <sup>3</sup> Wm. G. Hoover, *Computational Statistical Mechanics* (Elsevier, New York, 1991).
- <sup>4</sup> C. P. Dettmann and G. P. Morriss, "Hamiltonian Formulation of the Gaussian Isokinetic Thermostat", *Physical Review E* **54**, 2495-2500 (1996).
- <sup>5</sup> C. Braga and K. P. Travis, "A Configurational Temperature Nosé-Hoover Thermostat", *Journal of Chemical Physics* **123**, 134101 (2005).
- <sup>6</sup> C. Braga and K. P. Travis, "Constant Pressure Molecular Dynamics", *Journal of Chemical Physics* **124**, 104102 (2006).
- <sup>7</sup> K. P. Travis and C. Braga, "Configurational Temperature and Pressure Molecular Dynamics: Review of Current Methodology and Applications to the Shear Flow of a Simple Fluid", *Molecular Physics* **104**, 3735-3749 (2006).
- <sup>8</sup> L. D. Landau and E. M. Lifshitz, *Statistical Physics*, equation 33.14 (McGraw-Hill, New Jersey, 1958).
- <sup>9</sup> Wm. G. Hoover and C. G. Hoover, "Hamiltonian Dynamics of Thermostated Systems: Two-Temperature Heat-Conducting  $\phi^4$  Chains" *Journal of Chemical Physics* (in press, 2007).
- <sup>10</sup> W. G. Hoover and H. A. Posch, "Direct Measurement of Equilibrium and Nonequilibrium Lyapunov Spectra", *Physics Letters A* **123**, 227-230 (1987).
- <sup>11</sup> G. Benettin, L. Galgani, A. Giorgilli, and J. M. Strelcyn, "Tous les Nombres Caractéristiques de Lyapounov sont Effectivement Calculables", *Comptes Rendus de l'Académie des Science Paris* **286A**, 431-433 (1978).
- <sup>12</sup> H. A. Posch and W. G. Hoover, "Chaotic Dynamics in Dense Fluids", in *Proceedings of the Europhysics Liquid State Conference on Liquids of Small Molecules, Santa Trada, Italy, 1987*, edited by M. Nardone (European Physical Society, 1987), Volume **11G**, page 17.
- <sup>13</sup> B. L. Holian, W. G. Hoover, and H. A. Posch, "Resolution of Loschmidts Paradox: The Origin

- of Irreversible Behavior in Reversible Atomistic Dynamics”, *Physical Review Letters* **59**, 10-13 (1987).
- <sup>14</sup> Wm. G. Hoover, *Time Reversibility, Computer Simulation, and Chaos* (World Scientific, Singapore, 1999 and 2001).
- <sup>15</sup> Wm. G. Hoover, C. G. Hoover, H. A. Posch, and J. A. Codelli, “The Second Law of Thermodynamics and Multifractal Distribution Functions: Bin Counting, Pair Correlations, and the [Definite Failure of the] Kaplan-Yorke Conjecture”, *Communications in Nonlinear Science and Numerical Simulation* **12**, 214-231 (2007).
- <sup>16</sup> Wm. G. Hoover, K. Boercker, and H. A. Posch, “Large-System Hydrodynamic Limit for Color Conductivity in Two Dimensions”, *Physical Review E* **57**, 3911-3916 (1998).
- <sup>17</sup> H. A. Posch and Wm. G. Hoover, “Lyapunov Instability of Classical Many-Body Systems”, *Journal of Physics: Conference Series* **31**, 9-17 (2006).
- <sup>18</sup> L. B. Lucy, “A Numerical Approach to the Testing of the Fission Hypothesis”, *The Astronomical Journal* **82**, 1013-1024 (1977).
- <sup>19</sup> Wm. G. Hoover and H. A. Posch, “Entropy Increase in Confined Free Expansions *via* Molecular Dynamics and Smooth-Particle Applied Mechanics”, *Physical Review E* **59**, 1770-1776 (1999).
- <sup>20</sup> Wm. G. Hoover and H. A. Posch, “Numerical Heat Conductivity in Smooth Particle Applied Mechanics”, *Physical Review E* **54**, 5142-5145 (1996).
- <sup>21</sup> H. A. Posch, Wm. G. Hoover, and O. Kum, “Steady-State Shear Flows *via* Nonequilibrium Molecular Dynamics and Smooth-Particle Applied Mechanics”, *Physical Review E* **52**, 1711-1720 (1995).
- <sup>22</sup> Wm. G. Hoover, *Smooth Particle Applied Mechanics; the State of the Art* (World Scientific, Singapore, 2006).
- <sup>23</sup> H. A. Posch and W. G. Hoover, “Simulation of Two-Dimensional Kolmogorov Flow with Smooth Particle Applied Mechanics”, *Physica A* **240**, 286-296 (1997).